Antenna Pattern Measurements of Weather Radars Using the Sun and a Point Source

JENS REIMANN AND MARTIN HAGEN

Institut für Physik der Atmosphäre, Deutsches Zentrum für Luft- und Raumfahrt, Weßling, Germany

(Manuscript received 14 September 2015, in final form 18 February 2016)

ABSTRACT

The sun is known to be a good target for weather radar calibration. In this paper high-resolution raster scans of the sun at high elevations will be used to derive the antenna pattern of weather radar, without being affected by beam propagation effects and reflections close to the earth's surface. It is shown that this pattern matches well to pattern measurements using a point source. Hence, a good estimation of the real antenna pattern can be derived using the sun.

Furthermore, formulas to extract undistorted antenna patterns from the sun, even at high-elevation angles, are derived. The signal processing required to achieve high sensitivity for the antenna pattern measurements will be described. Important parts of the antenna pattern—for example, sidelobes—become visible when using long integration times.

The polarimetric receiver channel cross-correlation coefficient is proposed as a figure of merit of the cross-polar isolation of the antenna and hence the cross-polar pattern. The results are also compared to point source measurements. This illustrates how an unpolarized signal source like the sun can be used to derive polarimetric variables.

1. Introduction

It is widely accepted that the sun can be used for calibration of weather radars. It can be used to check the antenna alignment (Huuskonen and Holleman 2007) and to track receiver stability (Holleman et al. 2010a,b). An extended discussion of antenna calibration by means of the sun can also be found in Tapping (2001) and Free et al. (2007).

Measurements of the sun and other astronomic targets have been performed in radio astronomy (Baars 1973) for a long time. Unfortunately, most cosmic sources with better characteristics than the sun (stable power, real point source) used in this community are too weak for weather radar observations. Nevertheless, some techniques developed in this area can be applied to weather radar measurements of the sun, too.

In this paper, dedicated raster scans are used to derive the antenna pattern, exemplarily shown for the polarimetric Doppler weather radar POLDIRAD. The scan strategy and signal processing will be described in detail. Especially, the correct data geodetic position mapping will be investigated in section 5. In section 7, the pattern derived from the sun and from a point source will be compared. It will be shown that the cross correlation between the receiver channels is a figure of merit for the cross-polar isolation of the antenna. This is of special interest due to the cross polarization inherently generated by (single) reflector antennas used in many weather radar systems. The effect of imperfect antennas was already analyzed in the beginning of polarimetric research weather radar (e.g., Metcalf and Ussailis 1984) and became again important when polarimetry became operation in the weather radar community (Zrnić et al. 2010).

2. Sun properties

Besides the visible light, the sun radiates in a wide frequency band. When calibrating radar using the sun, the radar is in fact used as a radiometer. The radar transmitter will not be used, as no echo from the sun is expected (the pulse travel time is >15 min due to the distance between the earth and the sun). Hence, only the radar receiver path can be calibrated using this technique. For a calibration of the whole system,

Corresponding author address: Jens Reimann, Institut für Physik der Atmosphäre, Deutsches Zentrum für Luft- und Raumfahrt e.V., Münchener Straße 20, 82234 Weßling, Germany.
E-mail: jens.reimann@dlr.de

DOI: 10.1175/JTECH-D-15-0185.1

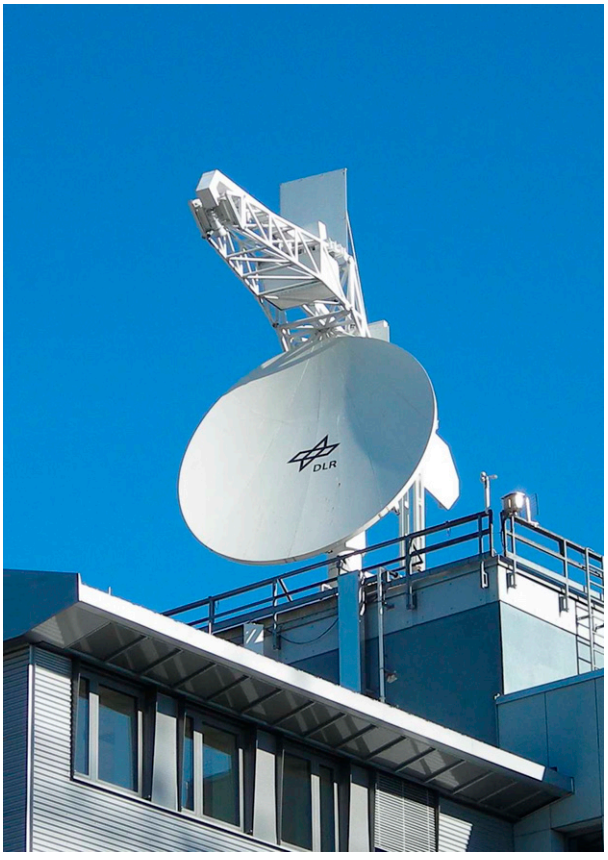

FIG. 1. POLDIRAD weather radar mounted on the DLR's Institute of Atmospheric Physics building.

including the transmitter, other techniques have to be exploited (e.g., a metallic sphere).

The sun radiation originates from physical processes that make it (nearly) white noise and virtually unpolarized for weather radar frequencies and beamwidths (Tapping 2001). The radiation intensity is slightly varying on a daily basis, depending on the sun's activity. These changes are tracked by various stations across the globe and can be used as reference values during absolute power calibration (e.g., U.S. DOC 2015; DRAO 2015).

The sun can be assumed to be in the far-field region for all operative weather radar antennas, but it is not a point source. Rather, it is a homogeneous disc (Baars 1973) with a diameter of approximately 0.57° (Holleman et al. 2010b) for radiowave emission. The position of the sun at the sky is well known and can be calculated with precision much better than 0.001° (e.g., Reda and Andreas 2004).

For consistency, we treat the noiselike emission from the sun as the desired signal within the whole paper. All other energy reaching the receiver is treated as (unwanted) noise (e.g., background radiation, thermal noise). Intentionally, this stands in contrast with the standard definition of noise in the weather radar community, where also the radiation from the sun is undesired.

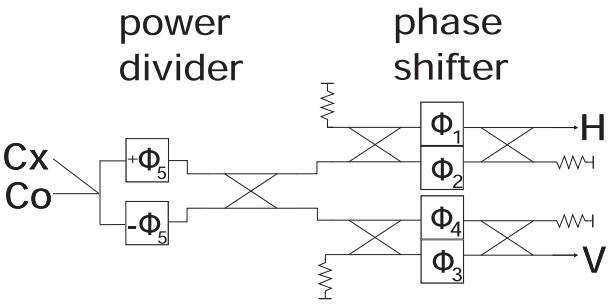

FIG. 2. Scheme of the POLDIRAD polarization network, consisting of phase shifter Φ_1–Φ_5.

3. Polarimetric C-band radar POLDIRAD

POLDIRAD (Fig. 1) is the C-band (precisely 5.504 GHz) research radar of the German Aerospace Center [Deutschen Zentrums für Luft- und Raumfahrt (DLR e.V.)] located in Oberpfaffenhofen (see Schroth et al. 1988). It consists of a 15-ft (about 4.5 m) offset parabolic antenna (equal to about 1° beamwidth), a magnetron transmitter, and a modernized Selex ES Gematronik GDRX digital receiver. A special feature of the radar is its polarization network, which allows for defining the receive and transmit polarization for each radar pulse. Unfortunately, this device adds polarization dependent about 2.5-dB loss to the receive/transmit path and breaks reciprocal system behavior. Hence, only the radar receiver can be characterized using the sun without any chance to derive properties of the transmit path.

a. *Polarization features*

The POLDIRAD is a very advanced system concerning its polarization abilities. A polarization network (Fig. 2), consisting of high-power ferrite phase shifters, allows the radar to transmit and receive in nearly every polarization basis. In a variable power divider section, the transmit pulse is split into two quantities using a magic tee. Both signal paths are phase shifted (Φ_5) in respect to each other and recombined. In the following phase shifter section (Φ_1–Φ_4), the horizontal and vertical signals are again phase shifted and then injected into an orthomode transducer at the antenna feed. In receive mode the signal is split into a copolar (Co) and a cross-polar (Cx) channel using the magic tee. Any polarization, including elliptical ones, can be transmitted and used for reception.

b. *Scan strategy*

Dedicated sun scans are feasible on POLDIRAD since it is used for research application only and is not in

TABLE 1. Scan parameters used for sun measurements.

Receiver bandwidth	2.4 MHz
PRF	1000 Hz
Azimuth averaging	600 pulses
Sampling range	30–90 km
Sampling resolution	30 m (oversampled)
No. of range samples	2000
Scan type	PPI
Scan position	Centered around the sun
Azimuth sampling range	±4°
Elevation sampling range	±2°
Antenna rotation speed	0.3 s^{-1}
No. of elevations	90
Scan time	~30 min

continuous operation. This allows for optimized scan strategy with adjusted parameters, for example, a small range sampling interval and very slow antenna rotation speed. Common scan parameters are listed in Table 1. The antenna is moved to raster a box around the actual sun position using several PPIs. This can last up to 30 or 45 min, depending on the averaging count. Since the sun is moving along the sky within this time interval, the scan box is defined in a way that the sun is captured throughout the whole scan. The time stamp for each radar pulse is used to derive the relative position between the antenna and the sun for each recorded data point.

4. Signal processing

The signal processing of POLDIRAD can be completely adapted to the desired research task, starting from the sampling interval over filtering and averaging applied down to product generation. A special signal processing chain is set up for sun scans that is adapted to the characteristics of the sun signal. The algorithms applied nearly completely differ from the ones used for weather observation; for example, clutter filtering, which might mistakenly remove parts of the desired signal, is omitted. Since no range resolution is required (the radar is operating as a radiometer), the signal processor is already averaging the signal along the whole range for data reduction.

a. Signal averaging

The main challenge when measuring the sun is sensitivity. The signal-to-noise ratio (SNR) can be enhanced by incoherent averaging. The (incoherent) averaging gain in linear scale is given by

$$g_{\text{avg}} = \sqrt{N}, \tag{1}$$

where N is the number of independent samples. Since the sun radiates white noise for typical weather radar frequencies, every sample can be assumed as independent and with equal variance. An extended measurement time pays off for an increased averaging gain.

Several techniques can be used to gather a large number of independent samples. First of all, the maximum number of range gates supported by the signal processor should be used (e.g., 2000 range gates for POLDIRAD). This is supported by selecting the smallest range gate length, which is equivalent to the highest sampling rate, and the smallest pulse length corresponding to the large filter bandwidth. Sampling times shorter than 1/Bandwidth used in this setup result in not completely independent samples and hence less averaging gain than expected from Eq. (1). Since the radar operates receive polarization only, there is no range dependency and each range gate can be considered as an independent sample of the sun's radiated signal. One data point consists of the range- and azimuth-averaged receiver samples (see Table 1) representative of the appropriate antenna pointing.

Only incoherent averaging is possible for the noiselike sun radiation using a single receiver. Only the amplitude/power of the receiver channels is used, while the phase is discarded. Besides this, the co–cross correlation between the receiver channels can be calculated. The correlation is a special case of coherent averaging. It is possible, as the receiver channels are coherent to each other. Hence, a signal present in both chains can be found by correlation. In contrast to the incoherent averaging of a single signal, the phase differences between two channels can also be used.

b. Noise estimation

Background noise estimating is probably the most crucial part of high-sensitivity sun radiation measurements. In our case the term *background noise* is defined as the signal seen at the receiver without contributions from the sun. This noise energy has to be subtracted from the measurement data to remove its effect. Very good noise samples are necessary for optimal performance. The noise sample size has to be at least as large as the averaging count N of the measurement data to achieve the same standard deviation, assuming that the sun radiation and background noise are ''white.''

This noise can be divided into noise from within the radar and noise from outside. The radar part is assumed to be invariant throughout the scan time, while the fluctuating noise is caused mainly from outside. The noise contribution received by the antenna is in general dependent on the antenna position, especially because it is dependent on the antenna elevation angle. While the noise temperature of the sky is between 2.7 K (empty sky) and 15 K (galactic plane; Baars 1973), the radiation from the earth is assumed to be about 290 K (blackbody radiator, approximately 17°C). The noise temperature can be converted to noise power using

$$P = kTB, \tag{2}$$

where k is the Boltzmann constant ($\approx 1.38 \times 10^{-23}\,\mathrm{J\,K^{-1}}$), T is the noise temperature, and B is the bandwidth of the system. Note that noise from the earth is 20–100 times stronger than the radiation from the sky.

Although high-directivity antennas are used for weather radars, energy entering from all directions in a virtual sphere around the antenna is collected. The angle-dependent antenna sensitivity to emission is described by the antenna radiation pattern. The whole power absorbed by the antenna is the integral over the radiation pattern and the signal energy from the specific direction. The main beam is most sensitive to radiation and often assumed to be the only source of signal power. Usually, additional high peaks appear near the main beam direction in the antenna pattern of reflector antennas, which are called 1st, 2nd, . . . , sidelobes. Since the radiation emitted by the earth is much stronger than the radiation from the sky, sidelobes hitting the ground can contribute significantly to the energy received by the whole antenna. This contribution is obviously mainly a function of the elevation angle. The background noise can also change over azimuth when mountains, buildings, or other *hot* obstacles are near the radar.

For high-elevation angles (>15°–20°), one noise sample is representative for a whole scan, because the first (and generally strongest) sidelobes are already pointing toward the sky and off the earth surface. For lower-elevation angles, it is beneficial to take noise samples when the antenna is pointing away from the sun while box scanning. In case very high averaging gain is needed, an additional noise scan can be performed, which virtually doubles the scan time. This noise scan uses the fact that the sun is moving over the sky, and the same sky region can be scanned earlier or later without the sun present. Achievable sensitivity when using an additional noise scan is only limited by the available scan time, the sun-position-dependent noise contributions (e.g., indirect radiation, change in surface temperature during scan), and system stability.

c. Derived quantities

For operational monitoring of the stability of the radar system, it is sufficient to analyze copolar and cross-polar power (e.g., Holleman et al. 2010a). However, additional parameters shown below can be derived (Figs. 4–6). The channel offset can be derived from the sun radiation, as the signal level at the antenna is supposed to be the same. This holds for any polarization basis and is a consequence of the unpolarized nature of the sun radiation. Furthermore, the reasonable assumption is made that both receiver paths have the equal bandpass characteristic. Violating this assumption would make the channel offset dependent on the received signal. The channel offset measurement involves the whole receiver chain and includes also the antenna. Keeping in mind that a noise component from within the radar is superposed, the signal seen at the receiver can be modeled,

$$P_{\mathrm{Co/Cx}} = P_{\mathrm{In}} \times g_{\mathrm{Co/Cx}} + \overline{\mathrm{noise}_{\mathrm{Co/Cx}}}, \tag{3}$$

where P_{In} is the power received by the antenna for the co- or cross-polar channel in linear units, $\overline{\mathrm{noise}_{\mathrm{Co/Cx}}}$ is the channel-dependent mean noise, $g_{\mathrm{Co/Cx}}$ is the channel gain, and $P_{\mathrm{Co/Cx}}$ is the power present at the analog-to-digital conversion (ADC) input port. No further perturbations are assumed in the digital part of the receiver chain.

After dividing both equations and reordering, it follows that

$$\frac{P_{\mathrm{Cx}}}{P_{\mathrm{Co}}} = \frac{g_{\mathrm{Cx}}}{g_{\mathrm{Co}}}\left(1 - \frac{\overline{\mathrm{noise}_{\mathrm{Co}}}}{P_{\mathrm{Co}}}\right) + \frac{\overline{\mathrm{noise}_{\mathrm{Cx}}}}{P_{\mathrm{Co}}}. \tag{4}$$

For $P_{\mathrm{Co}} \gg \overline{\mathrm{noise}_{\mathrm{Co/Cx}}}$, the power ration is equal to the gain ration, which is in logarithmic scale the receiver offset:

$$10\log_{10}\left(\frac{g_{\mathrm{Cx}}}{g_{\mathrm{Co}}}\right) = 10\log_{10}(g_{\mathrm{Cx}}) - 10\log_{10}(g_{\mathrm{Co}}). \tag{5}$$

For $P_{\mathrm{Co}} \approx \mathrm{noise}_{\mathrm{Co/Cx}}$, the ratio $P_{\mathrm{Cx}}/P_{\mathrm{Co}} \approx 1 = 0\,\mathrm{dB}$, which means no gain offset.

Each tuble of copolar and cross-polar power with sufficient high SNR received by the sun represents an estimate of the receiver channel offset. In a plot of copolar power versus cross-polar power, each of these tubles (a tuble is list of elements consisting of copolar and cross-polar power each) form a data point and the slope of a linear fit within the high-SNR region can be used as a stable estimation of the receive channel offset (see Fig. 3). The high-SNR region identified by its constant slope can also be estimated from the data itself.

Furthermore, the correlation coefficient ρ between both polarimetric receiver channels can be calculated using

$$\rho = \frac{\sum \underline{S_{\mathrm{Co}}}\,\underline{S_{\mathrm{Cx}}^{*}}}{\sqrt{\sum \underline{S_{\mathrm{Co}}^{2}} \sum \underline{S_{\mathrm{Cx}}^{2}}}}, \tag{6}$$

where $\underline{S_{\mathrm{Co}}}$ and $\underline{S_{\mathrm{Cx}}}$ are the complex samples of the copolar and cross-polar channels, respectively. This quantity describes the similarity between the signals in both channels. Since the signal received by the radar (Fig. 4) is unpolarized noise, the magnitude of the correlation coefficient should be zero for an infinite number of samples. It was found that several hundred thousand samples are needed to get sufficiently small correlation values (e.g., 0.01; see scale in Fig. 5) for further analysis.

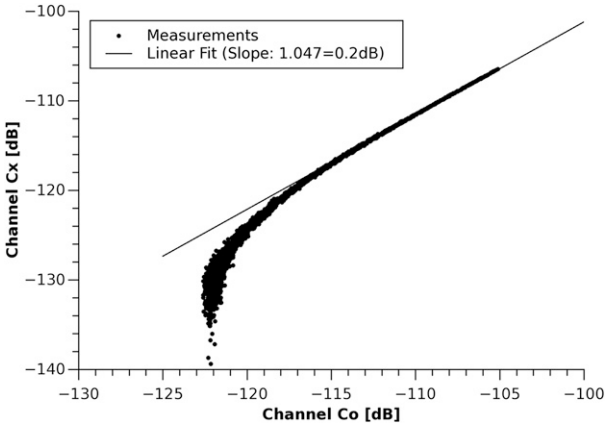

FIG. 3. Example of stable estimation of the receive channel offset from power samples received by the sun.

The magnitude of the correlation coefficient will rise if there is a similarity between the two channels data, for example, due to polarimetric cross coupling in the antenna. The angle-dependent pattern of the correlation coefficient (Figs. 5 and 6) indicates that the antenna is the source of signal coupling, not the receiver chains. The correlation phase will be the coupling phase.

A logarithmic value of power similarity can be derived by

$$\Sigma = 20 \log_{10} |\rho|, \tag{7}$$

which will be shown in section 7 to be similar to the power difference between the copolar and cross-polar signals.

5. Position mapping

When performing raster scans, appropriated data visualization is needed. Besides the antenna angles, the sun position has to be known. A good source is the solar position algorithm (SPA) from the U.S. National Renewable Energy Laboratory (Reda and Andreas 2004). It provides excellent precision and is available as program source code.

Typically, elevation-over-azimuth antenna positioners are used for weather radar. In this case subtracting angles to find the relative position between the antenna and the sun is only valid for low-elevation angles (e.g., Huuskonen and Holleman 2007). For elevation angles different from zero, a rotation of the radar antenna in azimuth with constant elevation angle does not describe a great circle on the sky sphere. The distortion still remains small for low-elevation angles.[1] In general, a more sophisticated approach has to be used.

[1] An extreme case occurs when rotating the azimuth axis of the radar antenna with elevation angle 90°: no movement of the radar beam on the sky is performed.

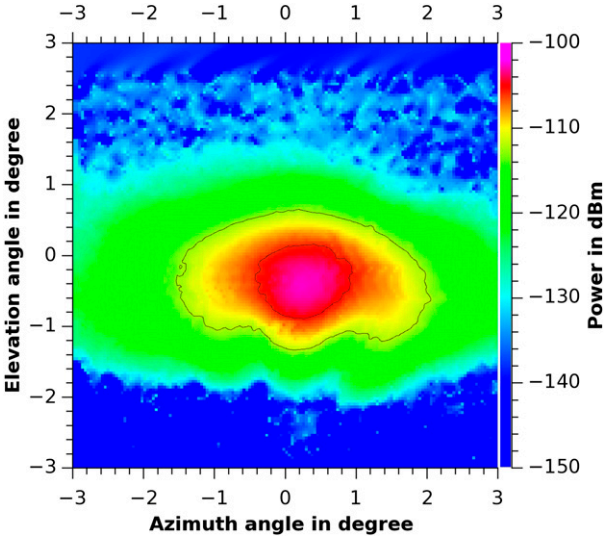

FIG. 4. Power received from the sun located at 260° in azimuth and 35° elevation at 1518 UTC 24 Jul 2012. Maximum power value is −104.2 dBm. The contours indicate the −3- and −10-dB power isolines.

An orthogonal coordinate system along great circles as shown in Fig. 7 is needed. Point O defines the origin of an imaginary sphere around the antenna on which point A defines the main beam direction. The circle C_3 would be the trace of the main beam when rotating the antenna in azimuth. The position of the sun is indicated by point S. The relative position δEl and δAz are found from the vertex foot point V, which is orthogonal to the great circles C_1 through the sun and the parallel circle C_2

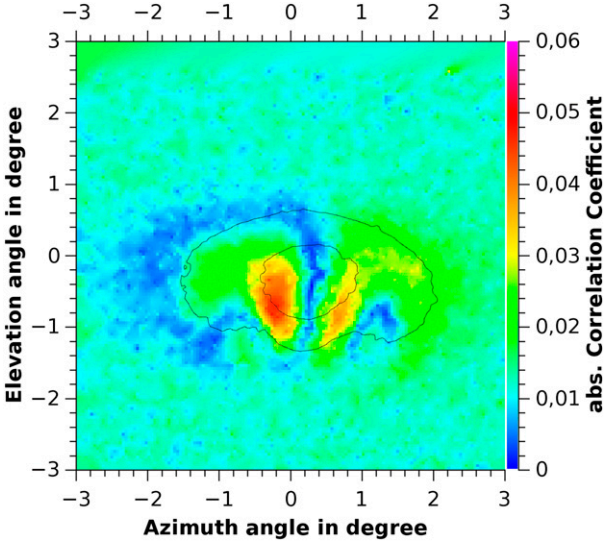

FIG. 5. Magnitude of the polarimetric correlation coefficient for the same measurement as in Fig. 4. The contours indicate the −3- and −10-dB power isolines.

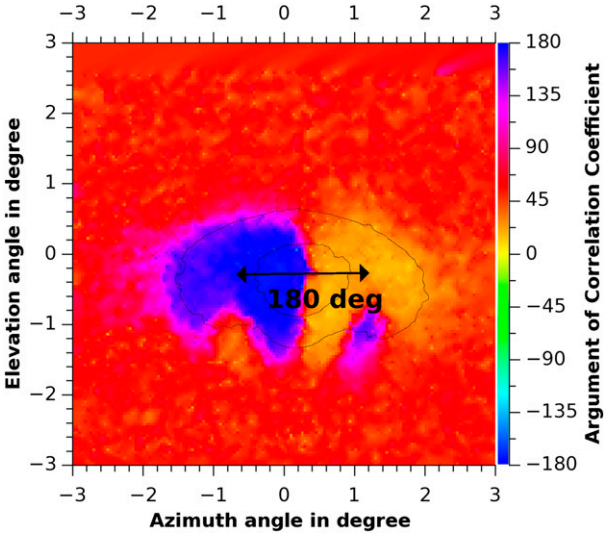

FIG. 6. Phase of the polarimetric correlation coefficient for the same measurement as in Fig. 4. The contours indicate the −3- and −10-dB power isolines.

through the antenna. Term C_2 is in general not a great circle,

$$\sin(\delta\mathrm{El}) = -\cos(\mathrm{El_{ant}})\cos(\mathrm{Az_{sun}} - \mathrm{Az_{ant}}) \times \sin(\mathrm{El_{sun}}) + \sin(\mathrm{El_{ant}})\cos(\mathrm{El_{sun}}), \quad (8)$$

$$\cos(\delta\mathrm{El})\sin(\delta\mathrm{Az}) = \cos(\mathrm{El_{ant}})\sin(\mathrm{Az_{sun}} - \mathrm{Az_{ant}}), \quad (9)$$

and

$$\cos(\delta\mathrm{El})\cos(\delta\mathrm{Az}) = \cos(\mathrm{El_{ant}})\cos(\mathrm{Az_{sun}} - \mathrm{Az_{ant}}) \times \cos(\mathrm{El_{sun}}) + \sin(\mathrm{El_{ant}})\sin(\mathrm{El_{sun}}). \quad (10)$$

The calculation can be derived from Fig. 8, where point A described by $\mathrm{Az_{ant}}$ and $\mathrm{El_{ant}}$ is the azimuth and elevation angle of the radar antenna, respectively; and point S represents the sun with its angles $\mathrm{Az_{sun}}$ and $\mathrm{El_{sun}}$. The symbols δEl and δAz depict the correct display angles to be evaluated. Therefore, an auxiliary triangle N–P–A is defined where ***N*** is the North Pole or zenith. Point P is the North Pole of the $\mathrm{El_{sun}}$ rotated system with equator C_1.

Two sides $\mathrm{El_{sun}}$ and $90°-\mathrm{El_{ant}}$ and one angle $180°-(\mathrm{Az_{sun}} - \mathrm{Az_{ant}})$ are known for this triangle. One side $(90°-\delta\mathrm{El})$ and one angle (δAz) can be calculated using Eqs. (8)–(10). This mathematical statement is similar to the calculation performed in astronomy to transfer positions in/from the ecliptic.

Plotting data using the δEl and δAz positions creates an undisrupted image of the sun–antenna convolution for further analysis (e.g., Fig. 4).

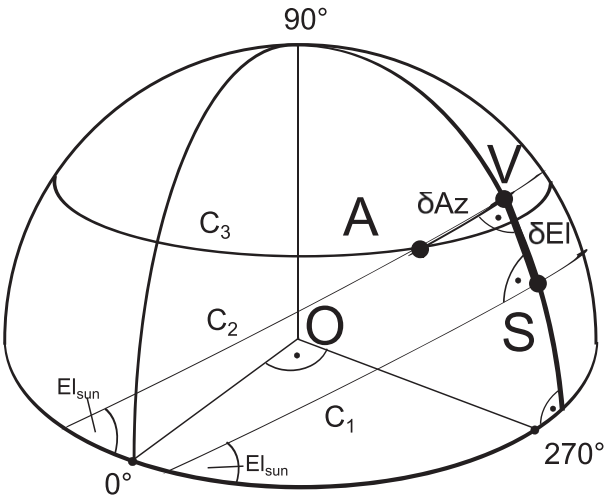

FIG. 7. Definitions required for creating an orthogonal coordinate system on a sphere.

6. Effect of pedestal tilting

It was found from sun measurements that the POLDIRAD pedestal was tilted. This was caused by the imperfect reassembling of the radar antenna pedestal after the Convective and Orographically Induced Precipitation Study (COPS) field campaign (Wulfmeyer et al. 2008).

The retrieved antenna alignment offset derived from the sun scans varied for different positions of the sun during the course of a day. In fact, the elevation was too low in the morning and too high in the evening. Since high-resolution sun scans are time consuming, further investigation was done by a spirit level gauge. Figure 9 shows these measurements of the tilting. The gauge was mounted orthogonal to the pedestal along the azimuth direction of the reflector. By rotation of the antenna, the

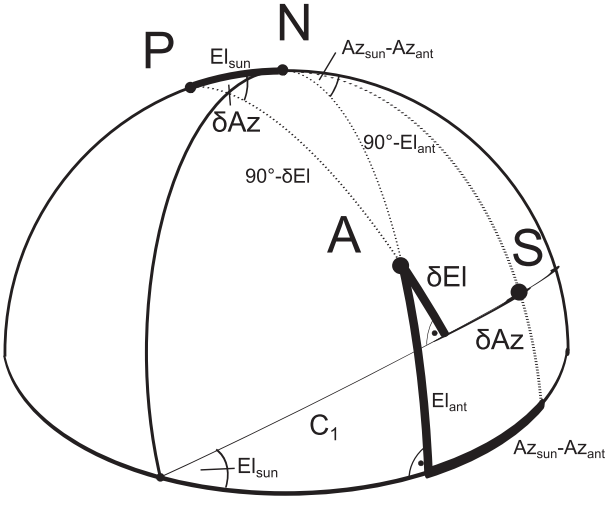

FIG. 8. Illustration of the coordinate system transformation.

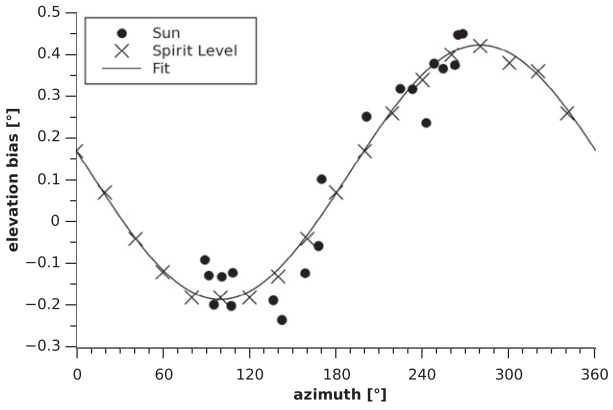

FIG. 9. Antenna tilt estimated from spirit gauge and sun measurements. The (arbitrary) offset of the spirit gauge measurements was adjusted to fit the sun elevation angle.

leveling becomes maximum or minimum perpendicular to the tilting direction. Furthermore, this setup is independent of the elevation angle of the reflector. For the retrieval the absolute level is not required. The 90° shift in azimuth caused by the gauge mounting was already removed and the absolute measurement values were adjusted to fit the sun measurements in Fig. 9. It is also obvious that the pointing error measured using the sun correlates with the azimuth position. From a fit through the gauge measurement, the tilt was determined to 0.3° (amplitude of the sine fit) at 280° azimuth (maxima of the sine fit). After mechanical correction the tilt was compensated to less than 0.1°, which was the measurement accuracy.

7. Antenna pattern analysis and comparison to point source

For an engineering antenna radiation pattern measurement, a point source is used. Unfortunately, the sun has a nonzero angular size. Hence, the received signal is the convolution of the sun disc and the antenna pattern. The sun can be treated as a homogeneous disc with an approximate diameter of 0.57° for C-band radars with an approximately 1° beamwidth. In this special case the convolution results in a spatial averaging of the antenna pattern. The resulting broadening caused by the sun is predicted to be approximately of 1% using the formulas from Baars (1973).

Besides the sun measurements, tests using a point source were performed for comparison. For these tests a device called a polarimetric active radar calibrator (PARC) was used, which is an internal DLR development designed for calibration of POLDIRAD (Reimann 2013). This PARC is used only as a signal generator (up to +16-dB*m* transmit power) to provide a known and constant signal source with a beamwidth of

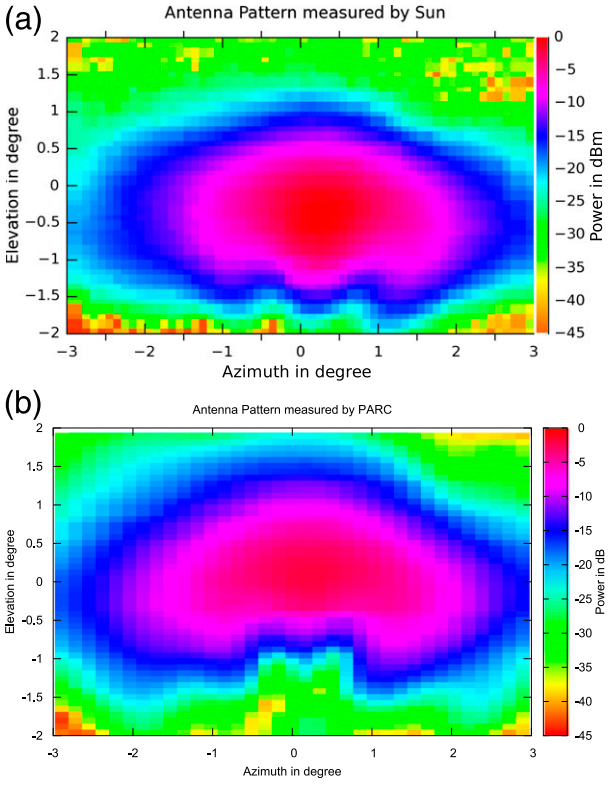

FIG. 10. Comparison of antenna pattern derived from sun scans and from a point source. (a) Antenna pattern derived from sun scans. (b) Antenna pattern measured with PARC.

about 20°. The signal power was chosen to produce an SNR at the radar better than 40 dB. Unfortunately, the PARC system could not be placed in the far-field region due to the lack of a suitable location. The distance was only approximately a third of the required distance of 750 m. Referring to (Balanis 2008, p. 12) this fact will mainly lead to stronger sidelobes and less pronounced nulls in the pattern, which should be acceptable for the shown comparison.

The box scan data from the PARC are shown in Fig. 10b, while the data from the sun are shown in Fig. 10a (scaled to the same resolution). The complicated pattern shape of the offset antenna system is clearly visible in both figures. It is far away from the rotational symmetry assumption often used in modeling the antenna pattern. Nevertheless, both measurements are similar.

The cross-polar lobes from the sun measurements (Fig. 5) match well the theoretical pattern (Rudge and Adatia 1978, section III). The phase difference between the copolar and cross-polar signals is shown in Fig. 6. The phase difference between the cross-polar lobes matches well the expected 180° (see Rudge and Adatia 1978).

A direct comparison of the azimuth antenna pattern recorded with the point source PARC and the derived one from the sun is shown in Fig. 11. The azimuth cut

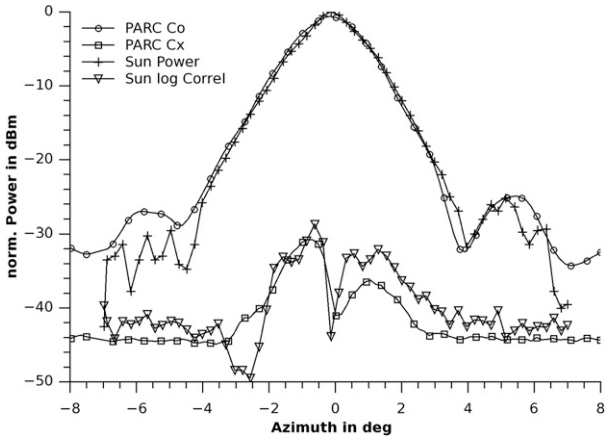

FIG. 11. Antenna azimuth cut comparison of the sun and point source.

position for the sun was chosen to be the expected main beam direction; the PARC cut was also set to the middle of the resulting pattern. The minor differences in the copolar main lobe are caused by the slightly different cut position of both measurements and the averaging done by the sun. Remarkably, even the sidelobes estimated from the sun measurement, which are close to the noise level, fit well. It is also obvious that the logarithmic correlation magnitude Σ [see Eq. (7)] represents nicely the cross-polar signal derived from the PARC. This is also true for the correlation phase and the co–cross phase from the point measurements (not shown). A small imbalance of the cross-polar lobes is visible in both the PARC and sun measurements.

8. Conclusions

We presented a technique that uses the sun to derive the antenna pattern with high spatial resolution and high sensitivity. Yet, the first sidelobes of the high-gain antenna become visible. This part of the pattern is of high interest for weather radar application. The pattern retrieval from the sun is easier to perform than a distinct measurement setup. A comparison between the sun and point source measurements has shown coinciding results. The correlation coefficient between the two polarimetric channels is proposed to contain information about the cross-polar isolation and therefore the cross-polar antenna pattern, which was verified using the point source measurements.

It was also shown that for higher-elevation angles, a transformation of the coordinate system into the center of the sun is mandatory. The required formulas have been derived and were used throughout the presented analysis.

REFERENCES

Baars, J., 1973: The measurement of large antennas with cosmic radio sources. *IEEE Trans. Antennas Propag.*, **21**, 461–474, doi:10.1109/TAP.1973.1140521.

Balanis, C. A., 2008: *Modern Antenna Handbook*. John Wiley and Sons, 1704 pp.

DRAO, 2015: Solar radio flux report. Accessed 19 January 2015. [Available online at www.spaceweather.ca/sx-4-eng.php.]

Free, A. D., N. K. Patel, R. L. Ice, and O. E. Boydstun, 2007: WSR-88D ORDA antenna gain and beamwidth algorithms. *23rd Conf. on Interactive Information Processing Systems (IIPS) for Meteorology, Oceanography, and Hydrology*, San Antonio, TX, Amer. Meteor. Soc., P2.16. [Available online at https://ams.confex.com/ams/87ANNUAL/techprogram/paper_118481.htm.]

Holleman, I., A. Huuskonen, R. Gill, and P. Tabary, 2010a: Operational monitoring of radar differential reflectivity using the sun. *J. Atmos. Oceanic Technol.*, **27**, 881–887, doi:10.1175/2010JTECHA1381.1.

——, ——, M. Kurri, and H. Beekhuis, 2010b: Operational monitoring of weather radar receiver chain using the sun. *J. Atmos. Oceanic Technol.*, **27**, 159–166, doi:10.1175/2009JTECHA1213.1.

Huuskonen, A., and I. Holleman, 2007: Determining weather radar antenna pointing using signals detected from the sun at low antenna elevations. *J. Atmos. Oceanic Technol.*, **24**, 476–483, doi:10.1175/JTECH1978.1.

Metcalf, J. I., and J. S. Ussailis, 1984: Radar system errors in polarization diversity measurements. *J. Atmos. Oceanic Technol.*, **1**, 105–114, doi:10.1175/1520-0426(1984)001<0105:RSEIPD>2.0.CO;2.

Reda, I., and A. Andreas, 2004: Solar position algorithm for solar radiation applications. *Sol. Energy*, **76**, 577–589, doi:10.1016/j.solener.2003.12.003.

Reimann, J., 2013: On fast, polarimetric non-reciprocal calibration and multipolarization measurements on weather radars. Ph.D. dissertation, Technische Universität Chemnitz, 161 pp. [Available online at http://nbn-resolving.de/urn:nbn:de:bsz:ch1-qucosa-132088.]

Rudge, A. W., and N. A. Adatia, 1978: Offset-parabolic-reflector antennas: A review. *Proc. IEEE*, **66**, 1592–1618, doi:10.1109/PROC.1978.11170.

Schroth, A. C., M. Chandra, and P. F. Meischner, 1988: A *C*-band coherent polarimetric radar for propagation and cloud physics research. *J. Atmos. Oceanic Technol.*, **5**, 803–822, doi:10.1175/1520-0426(1988)005<0803:ABCPRF>2.0.CO;2.

Tapping, K., 2001: Antenna calibration using the 10.7 cm solar flux. Preprints, *Workshop on Radar Calibration*, Albuquerque, NM, Amer. Meteor. Soc., 32 pp.

U.S. DOC, 2015: Solar radio data. Accessed 19 January 2015. [Available online at ftp://ftp.swpc.noaa.gov/pub/lists/radio/.]

Wulfmeyer, V., and Coauthors, 2008: The Convective and Orographically-Induced Precipitation Study (COPS): The scientific strategy, the field phase, and research highlights. *Quart. J. Roy. Meteor. Soc.*, **137**, 3–30, doi:10.1002/qj.752.

Zrnić, D., R. Doviak, G. Zhang, and A. Ryzhkov, 2010: Bias in differential reflectivity due to cross coupling through the radiation pattern of polarimetric weather radars. *J. Atmos. Oceanic Technol.*, **27**, 1624–1637, doi:10.1175/2010JTECHA1350.1.